This is the accepted manuscript made available via CHORUS. The article has been published as:

Observation of topological surface states in the high-temperature superconductor MgB_{2}

Xiaoqing Zhou, Kyle N. Gordon, Kyung-Hwan Jin, Haoxiang Li, Dushyant Narayan, Hengdi Zhao, Hao Zheng, Huaqing Huang, Gang Cao, Nikolai D. Zhigadlo, Feng Liu, and Daniel S. Dessau

Phys. Rev. B **100**, 184511 — Published 21 November 2019

DOI: 10.1103/PhysRevB.100.184511

Observation of Topological Surface States in High Temperature Superconductor MgB_2

Authors
Xiaoqing Zhou[1*], Kyle N. Gordon[1], Kyung-Hwan Jin[2], Haoxiang Li[1], Dushyant Narayan[1], Hengdi Zhao[1], Hao Zheng[1], Huaqing Huang[2], Gang Cao[1], Nikolai D. Zhigadlo[3], Feng Liu[2,4], and Daniel S. Dessau[1,5*]

Affiliations
[1]*Department of Physics, University of Colorado at Boulder, Boulder, CO 80309, USA*
[2]*Department of Physics, University of Utah, Salt Lake City, UT 84112, USA*
[3]*Department of Chemistry and Biochemistry, University of Bern, CH-3012 Bern, Switzerland*
[4]*Collaborative Innovation Center of Quantum Matter, Beijing, 100084, China*
[5]*Center for Experiments on Quantum Materials, University of Colorado at Boulder, Boulder, CO 80309, USA*

Correspondence to: Xiaoqing.Zhou@Colorado.edu, Dessau@Colorado.edu

Abstract

Most topological superconductors known-to-date suffer from low transition temperatures (T_c) and/or high fragility to disorder and dopant levels, which is hampering the progress in this promising field. Here, utilizing a combination of Angle-resolved Photoemission Spectroscopy (ARPES) measurements and Density Functional Theory (DFT) calculations, we show the presence of a novel type of topological Dirac nodal line surface state on the [010] faces of the T_c=39K BCS superconductor MgB_2. This surface state should be highly tolerant against disorder and inadvertent doping variations and is expected to go superconducting via the proximity effect to the bulk superconductor that this state is intimately connected to. This would represent a new form of high temperature topological superconductivity.

Introduction

As its name suggests, a topological superconductor needs two essential ingredients: nontrivial topology and the superconducting order. Initially, the exploration of topological superconductivity was limited to the 5/2 quantum Hall state in electron gas systems[1,2,3] and p-wave superconductors such as Sr_2RuO_4[4, 5, 6], in which the chiral superconducting order parameter is topologically nontrivial by itself. However, these systems are extremely sensitive to disorder, very scarce in nature, and have transition temperatures well below liquid helium temperature – each of which imposes great difficulties in the exploration of topological superconductivity. The discovery of topological band structures[7,8] introduces an alternative and arguably more favorable recipe - that the "topological" part of a topological superconductor can be substituted by a topological surface state. In systems with both topologically nontrivial band-inversions and conventional s-wave superconducting gaps[9], the topological surface state can be gapped by the superconducting gap [10, 11, 12] through the proximity effect and enables topological superconductivity. To avoid the complications of interface physics, it is preferable to use a single system, such as the one discussed here.

To make a singular topological superconductor, researchers have devoted a great deal of effort into doping known bulk topological material, which has seen some success in materials such as Cu-doped Bi_2Se_3 [13, 14, 15]. However, given that the discoveries of high temperature superconductivity have been largely accidental, it is unclear how far this approach can go. Here we adopt an alternative approach by looking for topological surface states in known high temperature superconductors – and MgB_2 ranks high on this list. At ambient pressure, its superconducting transition temperature of 39 K[16] is the highest among conventional s-wave superconductors, and second only to certain members of the cuprate and pnictide family among all known superconductors. Very recently, a particularly promising candidate $FeTe_{1-x}Se_x$[17] was found in the family of pnictide high temperature superconductors, with a transition temperature of 14.5 K setting the current record. While this discovery is exciting, the required proximity of a very small (20 meV scale) spin-orbit-coupled gap to the Fermi energy means that the system should be highly sensitive to inadvertent doping variations.

Although MgB_2 as a high temperature superconductor has been extensively studied by many techniques including ARPES[18, 19, 20, 21, 22], its ability to harbor topological surface states has never been appreciated. In this work, we use a combination of first principle density functional

theory (DFT) calculations and Angle-Resolved-Photoemission Spectroscopy (ARPES) to look for topological surface states in MgB_2. Our DFT calculations[23] have predicted the existence of pairs of topological Dirac nodal lines[24] at the Brillouin zone boundaries, as well as topological surface bands that connect these nodal lines. The calculations further predict that the topological surface states should be robust against realistic doping variations, and readily gapped by the superconducting order, as expected by the intimate and inherent contact between the bulk superconducting states and the topological surface states.

Results

The key to the topological surfaces states are the topological Dirac nodal lines, with associated Dirac points on high symmetry cuts (highlighted by the arrows in the band-structure plot of Fig. 1c). As illustrated by Fig. 1d, the Dirac nodal line disperses across E_F in the k_z direction (normal to the honeycomb layers) over a few eV range, so that Dirac band crossings as well as the corresponding topological surface states will always be present at E_F for essentially any conceivable amount of doping or band-bending effects. As shown in Fig. 1b, the Dirac nodal lines predicted by the DFT calculation are located at the zone boundary of the 3D Brillouin zone along the K-H and K'-H' high symmetry lines that run along the z axis. Our calculations (see supplementary materials[25] and references[1,2] therein) show that each of these nodal lines in MgB_2 is wrapped by a Berry phase of π, i.e. they support a Z2 topology. Similar to the case in graphene, the K'-H' line can be regarded as the mirror image of the K-H, so the associated Berry phase for the K'-H' nodal line is $-\pi$ instead of π for the K-H nodal line.

Because of their k_z dispersion, the Dirac nodal lines can be best accessed from the side so that the dispersion is in the experimental plane – a geometry different from all previous ARPES experiments that studied the sample from the c-axis, which is also the natural cleavage face. For our experiment we cleaved the samples from the "side" (blue plane of Fig 1a and 1b) and performed ARPES on that thin [010] face – a challenging but achievable task. The cleaved surface viewed with a scanning electron microscope (see Fig. 2b) as well as an atomic force microscope (see supplementary materials[25] and references[3-8] therein) shows an atomically flat region, upon which high quality ARPES spectra were observed at 10 K. We measured the band dispersion along the momentum perpendicular to the cleavage face (k_x) by scanning the photon energy $h\nu$ from 30 eV to 138 eV along the Γ-K high symmetry line with linear s-polarization. Since at these photon energies the photon momentum is negligible, we have [26]

$$k_x \approx \sqrt{\frac{2m_e}{\hbar^2}(h\nu - \emptyset - E_B + V_0) - (k_y^2 + k_z^2)} \quad (1)$$

where $\emptyset = 4.3$ eV is the work function, E_B the binding energy, and $V_0 = 17\,eV$ the inner potential. This describes the ARPES spectra measured on a "spherical sheet", the radius of which is proportional to $\sqrt{h\nu - \emptyset - E_B + V_0}$. By stitching together many spectra taken over a wide range of photon energies from 30-138 eV, we reconstruct the iso-energy plots in the [001]-plane at $k_z = 0$, as shown in Fig. 2d to 2g. The data show a spectra consistent with previous ARPES studies on the [001] cleavage plane[18-22] (see supplementary materials[25]). This confirms that we are able to observe the proper bulk band structure of MgB_2 from the cleaved [010] plane. As illustrated in Fig. 2c, in our experimental geometry the K-H Dirac nodal line acts as a monopole of Berry phase and is neighbored by 3 of its "mirror-image" K'-H' lines with opposite charge, each of which has bulk bands accessible only under different experimental conditions (i.e. photon energies and experimental angles). We choose the photon energy $h\nu$ = 86 eV (black line in the panels), which allows us to directly access one of the K-H high symmetry lines by varying the k_z momentum axis.

To better investigate the Dirac nodal line, Fig. 3 focuses on the region near the high symmetry line K-H at $k_x \approx 8\pi/\sqrt{3}a$, $k_y = 4\pi/3a$ and $k_z \sim \pi/c$ to $2\,\pi/c$. As shown in Fig. 3a, on the projected surface Brillouin zone we should expect a 2D topological surface state (TSS) connecting a pair of 1D Dirac nodal lines with opposite charges[27], as any loop encircle the nodal lines will pick up a Berry phase of π or -π. This "water-slide" TSS is analogous to the flat "drumhead" surface state in Dirac nodal loop systems[28], but follows the dispersions of the nodal lines over a range of ~4 eV. Viewed from the sample projection (Fig. 3b), the topological surface states could connect the +π nodal line ($k_y = 4\pi/3a$) to the –π nodal line on the left ($k_y = 2\pi/3a$), or the one on the right ($k_y = 8\pi/3a$), but not both. As shown in Fig. 3b to 3i, we have excellent agreement between the DFT bulk band calculations and the ARPES iso-energy plots, in which the shifting touching point of an electron pocket and a hole pocket indicates non-trivial band crossings dispersing along K-H. Importantly, through momentum distribution curves (MDC) analysis (see supplementary materials[25]) we found an additional feature originating from the touching point that is absent from the DFT calculations of the bulk bands. It looks similar to a "Fermi arc" in Weyl semimetal[29], but persists for most binding energies ($E-E_F$) and connects

towards the -π bulk band crossing point at $k_y = 2\pi/3a$, even though the corresponding bulk bands are not experimentally accessible at 86 eV. These look like the TSS's drawn in Fig. 3b and we label them as such, though confirmation from an energy cut (Fig. 4) is still required.

To further confirm the topological nature of the surface state, in Fig. 4 we plot the dispersion along 5 cuts across the touching points (dotted lines in Fig. 3c). As the predicted Dirac nodal line should disperse along the *K-H* high symmetry cut, the band crossings should evolve continuously from below E_F to above E_F as shown in Fig. 1c. This is exactly what we observed, confirming the Dirac nodal line nature of these states. We directly overlay the DFT calculations of the bulk band dispersions (white dashed lines) with the ARPES spectra with no alteration of the masses or velocities, and a -0.5 eV offset in the DFT chemical potential (possibly due to the depletion of Mg or B atoms on the surface). The agreement is overall excellent, with the chemical potential shift indicative of extra electron charge leaving the cleaved surface. In particular, we stress that over a huge range of possible chemical shifts (such as those induced by unintentional doping), here the Dirac nodal lines dispersing along K-H guarantees Dirac points and topological surface states right at E_F, in sharp contrast to the case of $FeTe_{1-x}Se_x$ (see supplementary materials[25] for more discussions). In addition to the agreement with the bulk Dirac nodal line, the experiment shows some additional weak features which is captured by second derivative analysis (see supplementary materials[25]). As all bulk bands are accounted for, these should be of non-bulk origin, i.e. surface states. Most interesting of these are the ones highlighted in red that are observed to connect to the Dirac points in both energy space (Fig. 4) and momentum space (Fig. 3), with this effect observed over a wide range of energies and momenta. Away from the Dirac point its dispersion is much flatter than the bulk band in the s-p metal MgB_2. This is fully consistent with the existence of a topological surface state that we theoretically predicted to connect the Dirac points on this particular surface [23], and we label it as such. This state contrasts with a topologically trivial surface state (blue arrow) that is largely insensitive to the energy of the Dirac point as it disperses from cut to cut.

Discussion

These new topological surface states are expected to go superconducting via the proximity effect, which would make this material by far the highest transition temperature and most robust topological superconductor (TSC), and an excellent platform for a multitude of future studies. Even higher energy resolution ARPES than what we have carried out here could be utilized to

directly detect a superconducting gap in the TSS's, though this is non-trivial since the highest-resolution ARPES facilities are mostly laser-ARPES [30,31], which lack the ability to reach the relevant k-space locations. STM could also potentially be utilized to detect such a gap. Regardless, since the contact between the topological surface states with the bulk superconductivity is almost guaranteed to be near-ideal since the surface states are an intrinsic part of the electronic structure, this next step is highly likely to be realized. On the other hand, further explorations on MgB_2 still face quite a few of their own technical difficulties – that the (010) faces of single crystals are very small and difficult to work with, calling for atomically flat thin films[32] on the [010] face. A different probe, such as scanning tunneling microscopy[33], might provide vital insights into this exploration, too.

The observation of the topological surface state confirms the theoretical prediction of MgB_2 as a promising topological superconductor candidate. Given that there are no topological surface states near the Fermi energy in cuprate superconductors, and that the transition temperature in the best pnictides superconductors are not much higher, the potential topological superconductivity in MgB_2 would not only set the current record for T_c among topological superconductors but also approach the realistic limit. More important than the high T_c, however, is the fact that the topological surface state that is now expected in this material should be much less sensitive to disorder or dopant variations than in other topological superconductors, including the newly discovered state in $FeSe_{0.45}Te_{0.55}$[17]. MgB_2 thus has the best of these two ingredients, i.e. a high superconducting transition temperature and a robust topological surface state.

Last, the success in the conventional superconductor MgB_2 helps guide the hunt of topological superconductors to a different direction: since the topological surface state associated with Dirac nodal lines and loops seems to be more abundant[34] than that of high temperature superconductivity, we should optimize the weak link, and search for superconductors that have topological band structures or can be made topological.

Acknowledgments

We thank Drs. D. H. Lu, M. Hashimoto, and T. Kim for technical assistance on the ARPES measurements. We thank Dr. R. Nandkishore and Dr. Qihang Liu for useful discussions. The photoemission experiments were performed at beamline 5-2 of the Stanford Synchrotron

Radiation Lightsource and the Diamond Light Source beamline I05 (proposal no. SI17595). This work was funded by DOE project DE-FG02-03ER46066 (Colorado) and by the DOE project DE-FG02-04ER46148 (Utah). The Stanford Synchrotron Radiation Lightsource is supported by the Director, Office of Science, Office of Basic Energy Sciences, of the U.S. Department of Energy under Contract No. DE-AC02-05CH11231.

[1] Moore, G. and Read, N. Non-abelians in fractional quantum Hall effect, *Nucl. Phys. B* **360**, 362 (1981)

[2] Halperin, B. I. and Stern, A., Proposed Experiments to Probe the Non-Abelian ν = 5/2 Quantum Hall State, *Phys. Rev. Lett.* **96**, 016802 (2006)

[3] Bonderson, P., Kitaev, A. and Shtengel, K. Detect Non-Abelian Statistics in the ν = 5/2 Fractional Quantum Hall State, *Phys. Rev. Lett.* **96**, 016803 (2006)

[4] Das Sarma, S. Nayak, C. and Tewari, S., Proposal to stabilize and detect half-quantum vortices in strontium ruthenates thin films: Non-Abelian braiding statistics of vortices in a p_x+ip_y superconductor, *Phys. Rev. B 73, 220502(*R) (2006)

[5] Kallin, C., Chiral p-wave order in Sr_2RuO_4, *Rep. Prog. Phys.* **75**, 042501 (2012)

[6] Maeno, Y, Shunichiro Kittaka, Takuji Nomura, Shingo Yonezawa, and Kenji Ishida, Evaluation of Spin-Triplet Superconductivity in Sr_2RuO_4, *J. Phys. Soc. Jpn* **81**, 011009 (2012)

[7] Fu, L., Kane, C. L. and Mele, E. J, Topological Insulators in Three Dimensions, *Phys. Rev. Lett.* **98**, 106803 (2007)

[8] Kane, C. L. and Hasan, M. Z., Topological Insulators, *Rev. Mod. Phys.* **82**, 3045 (2010)

[9] Fu, L. and Kane, C. L, Superconducting Proximity Effect and Majorana Fermions at the Surface of a Topological Insulator, *Phys. Rev. Lett.* **100**, 096407 (2008)

[10] Wray, L. S., Su-Yang Xu, Yuqi Xia, Yew San Hor, Dong Qian, Alexei V. Fedorov, Hsin Lin, Arun Bansil, Robert J. Cava and M. Zahid Hasan, Observation of Topological Order in a Superconducting Doped Topological Insulator, *Nat. Phys.* **6**, 855 (2010)

[11] Wang, M. X., Liu, C. H., Xu, J. P., Yang, F., Miao, L., Yao, M. Y., Gao, C. L., Shen, C. Y., Ma, X. C., Chen, X., Xu, Z. A., Liu, Y., Zhang, S. C., Qian, D., Jia, J. F. and Xue, Q. K., The Coexistence of Superconductivity and Topological Order in the Bi_2Se_3 Thin Films, *Science* **336**, 52 (2012)

[12] Xu, S., Alidoust, N., Belopolski, I., Richardella, A., Liu, C., Neupane, M., Bian, G., Huang, S., Sankar, R., Fang, C., Dellabetta, B., Dai, W., Li, Q., Gilbert, J. M., Chou, F., Samarth, N. and Hasan, Z. M., Momentum-Space Imaging of Cooper Pairing in a Half-Dirac-Gas Topological Superconductor, *Nat. Phys.* **10**, 943 (2014)

[13] Y. S. Hor, A. J. Williams, J. G. Checkelsky, P. Roushan, J. Seo, Q. Xu, H. W. Zandbergen, A. Yazdani, N. P. Ong, and R. J. Cava,Superconductivity in $Cu_xBi_2Se_3$, and its Implications for Pairing in the Undoped Topological Insulator, *Phys. Rev. Lett.* 104, 057001 (2010)

[14] Fu, L. and Berg, E., Odd-Parity Topological Superconductors: Theory and Applications to $Cu_xBi_2Se_3$, *Phys. Rev. Lett.* **105**, 097001 (2010)

[15] Kriener, M., Segawa, K., Ren, Z., Sasaki, S and Ando, Y. Bulk Superconducting Phase with a Full Energy Gap in the Doped Topological Insulator $Cu_xBi_2Se_3$, *Phys. Rev. Lett.* **106**, 127004 (2011)

[16] Jun Nagamatsu, Norimasa Nakagawa, Takahiro Muranaka, Yuji Zenitani and Jun Akimitsu., Superconductivity at 39 K in Magnesium Diboride, *Nature,* **410**, 63 (2001)

[17] Peng Zhang, Koichiro Yaji, Takahiro Hashimoto, Yuichi Ota, Takeshi Kondo, Kozo Okazaki, Zhijun Wang, Jinsheng Wen, G. D. Gu, Hong Ding, Shik Shin, Observation of topological superconductivity on the surface of an iron-based superconductor, *Science,* **360**, 182 (2018)

[18] S. Tsuda, T. Yokoya, Y. Takano, H. Kito, A. Matsushita, F. Yin, J. Itoh, H. Harima, and S. Shin, Definitive Experimental Evidence for Two-Band Superconductivity in MgB_2, *Phys. Rev. Lett.* **91**, 127001 (2003)

[19] S. Souma, Y. Machida, T. Sato, T. Takahashi, H. Matsui, S.-C. Wang, H. Ding, A. Kaminski, J. C. Campuzano, S. Sasaki and K. Kadowaki, The origin of multiple superconducting gaps in MgB_2, *Nature* **423**, 65 (2003)

[20] S. Tsuda, T. Yokoya, T. Kiss, T. Shimojima, S. Shin, T. Togashi, S. Watanabe, C. Zhang, C. T. Chen, S. Lee, H. Uchiyama, S. Tajima, N. Nakai, and K. Machida, Carbon-Substitution dependent multiple superconducting gap of MgB_2: a sub-meV resolution photoemission study, *Phys. Rev. B* **72**, 064527 (2005)

[21] Y. Sassa, M. Månsson, M. Kobayashi, O. Götberg, V. N. Strocov, T. Schmitt, N. D. Zhigadlo, O. Tjernberg, and B. Batlogg, Probing two- and three-dimensional electrons in MgB_2 with soft x-ray angle-resolved photoemission*, Phys. Rev. B* **91**, 045114 (2015)

[22] Daixiang Mou, Rui Jiang, Valentin Taufour, S. L. Bud'ko, P. C. Canfield, and Adam Kaminski, Momentum dependence of the superconducting gap and in-gap states in MgB_2 multi-band superconductor, *Phys. Rev. B* **91**, 214519 (2015)

[23] Kyung-Hwan Jin, Huaqing Huang, Jia-Wei Mei, Zheng Liu, Lih-King Lim, Feng Liu, Topological Dirac-Nodal-Line Semimetal Phase in High-Temperature Superconductor MgB_2, *npj Comput. Mater*. 5, 57 (2019)

[24] Chiu, C. and Schnyder, A. Classification of reflection symmetry protected topological semimetals and nodal superconductors. *Phys. Rev. B*, **90**, 205136(R) (2014)

[25] See Supplemental Material at which includes further information on DFT method, sample growth and cleave details, additional ARPES spectra, and comparison to topological superconductivity in $FeTe_{1-x}Se_x$.

[26] Damascelli, A., Hussain, Z. and Shen, Z. X., Angle-Resolved Photoemission Studies of the Cuprate Superconductors, *Rev. Mod. Phys*. **75**, 473 (2003)

[27] Hyart, T., Ojajarvi, R and Heikkila, T. T., Two topologically distinct Dirac-line semimetal phases and topological phase transitions in rhombohedrally stacked honeycomb lattices, arXiv: 1709.05265 (2017), published J. Low Temp. Phys. **191**, 35-48 (2018)

[28] Y.-H. Chan, Ching-Kai Chiu, M. Y. Chou, and Andreas P. Schnyder, Topological Semimetals with line nodes and drumhead surface states, *Phys. Rev. B* **93**, 205132 (2015)

[29] Su-Yang Xu, Ilya Belopolski, Nasser Alidoust, Madhab Neupane, Guang Bian, Chenglong Zhang, Raman Sankar, Guoqing Chang, Zhujun Yuan, Chi-Cheng Lee, Shin-Ming Huang, Hao Zheng, Jie Ma, Daniel S. Sanchez, BaoKai Wang, Arun Bansil, Fangcheng Chou, Pavel P. Shibayev, Hsin Lin, Shuang Jia, M. Zahid Hasan, Discovery of a Weyl fermion semimetal and topological Fermi arcs, *Science* **349**, 613 (2015)

[30] J. D. Koralek, J. F. Douglas, N. C. Plumb, Z. Sun, A. V. Fedorov, M. M. Murnane, H. C. Kapteyn, S. T. Cundiff, Y. Aiura, K. Oka, H. Eisaki, and D. S. Dessau, Laser Based Angle-Resolved Photoemission, the Sudden Approximation and Quasiparticle-Like Spectra peak in $Bi_2Sr_2CaCu_2O_{8+\delta}$, *Phys. Rev. Lett.* **96**, 017005 (2006)

[31] Shimojima ,T., Okazaki ,K. and Shin ,S., Low-Temperature and High-Energy-Resolution Laser Photoemission Spectroscopy*, J. Phys. Soc. Jpn.* **84**, 072001 (2015)

[32] Xi, X. X., MgB_2 thin films, Super. Sc. Tech. **22**, 043001(2009)

[33] Dongfei Wang, Lingyuan Kong, Peng Fan, Hui Chen, Shiyu Zhu, Wenyao Liu, Lu Cao, Yujie Sun, Shixuan Du, John Schneeloch, Ruidan Zhong, Genda Gu, Liang Fu, Hong Ding, Hong-Jun Gao, Evidence for Majorana bound states in an iron-based superconductor, *Science* **362**, 333 (2018)

[34] Shuo-Ying Yang, Hao Yang, Elena Derunova, Stuart S. P. Parkin, Binghai Yan & Mazhar N. Ali, Symmetry demanded topological nodal-line materials, *Adv. Phys.* **3**, 1414631 (2018)

Figures and Tables

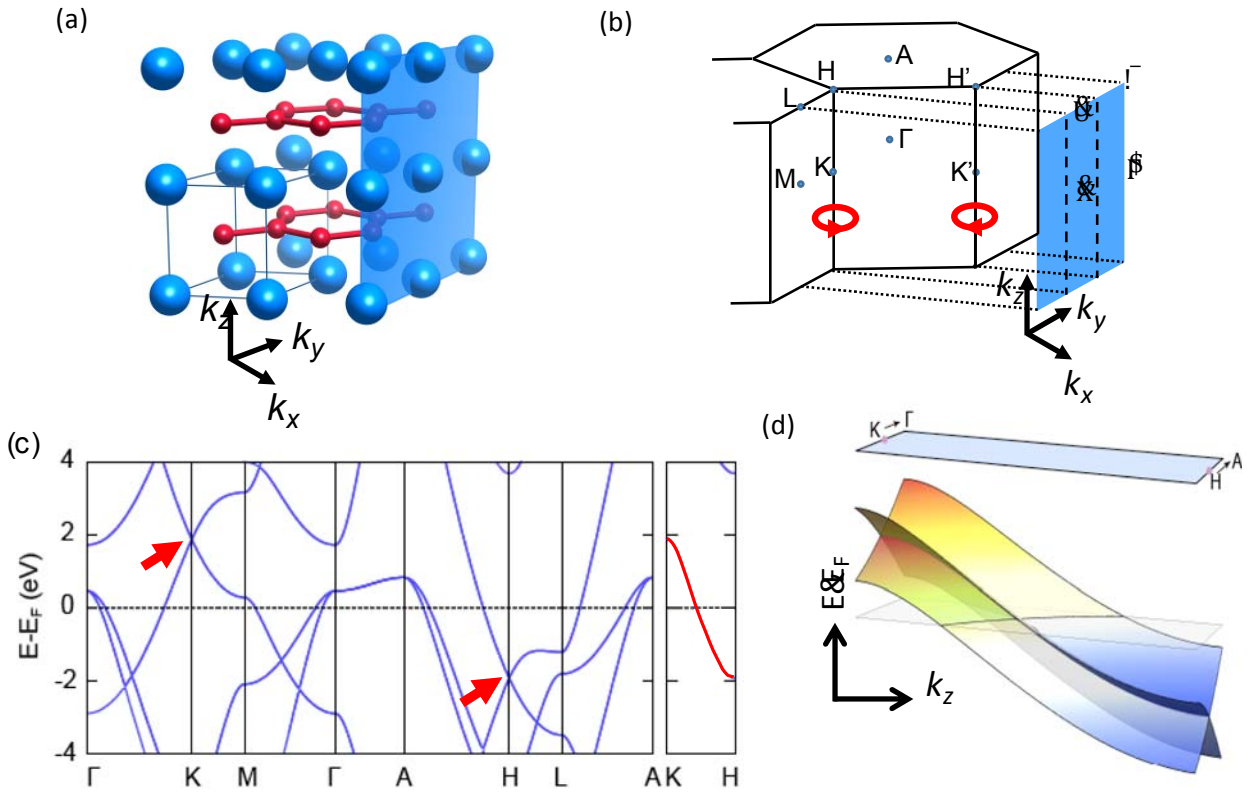

Fig. 1 a) Crystal structure of MgB_2 with hexagonal lattice in the ab-plane, determined by X-ray diffraction (XRD). The face of the edge-cleave is shown in blue, and the cleaved surface can be either Mg- or B-terminated. b) The 3D Brillouin zone and the projected "zigzag" [010] surface Brillouin zone (SBZ, shown as the blue sheet). High symmetry points K/H and K'/H' come in mirror-symmetric pairs, with Berry phase of π and $-\pi$ respectively. c) Calculated DFT bulk band structure along the high symmetry cut showing Dirac points (red arrows) along K-H. d) Illustration of a Dirac nodal line along K-H, with Dirac point exactly meeting E_F midway along the cut. The k_x direction is normal to the [010] surface and so is covered by varying photon energy, in our case from 30-140 eV.

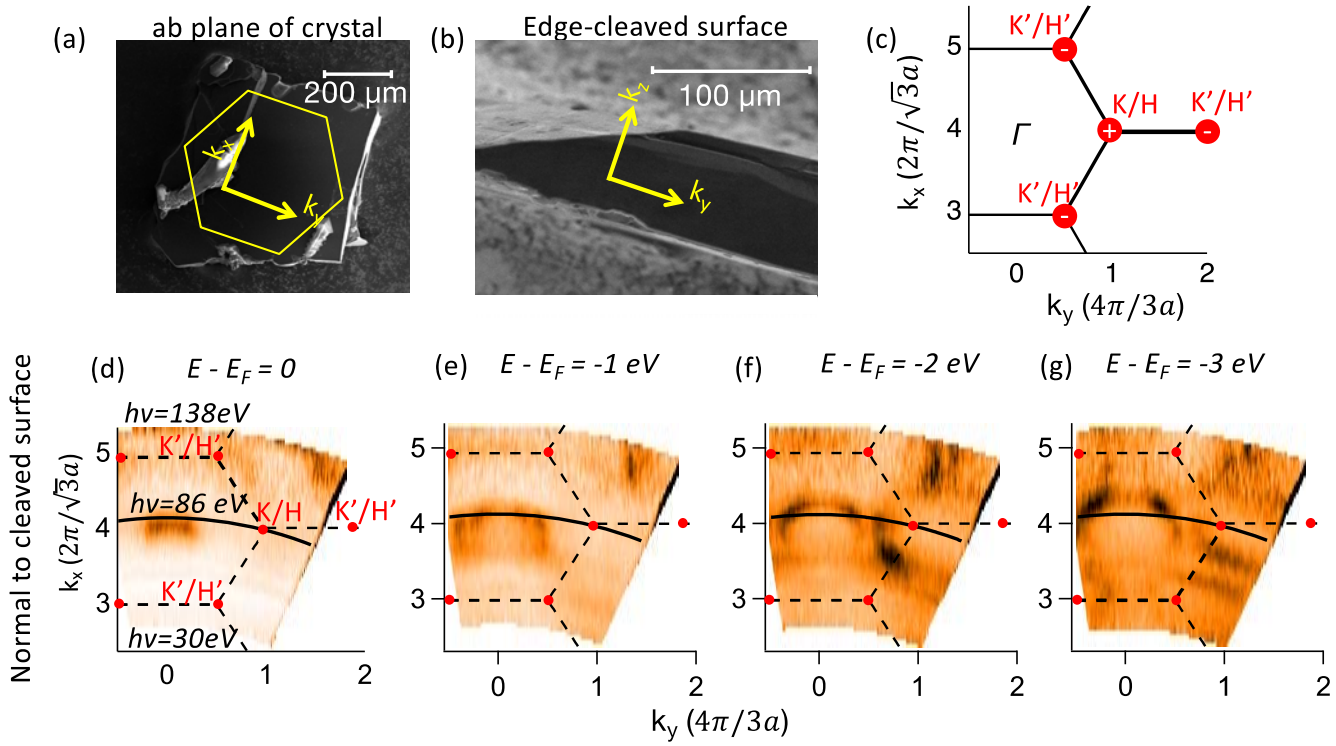

Fig 2. Edge-on ARPES gives in-plane bulk electronic structure. (a,b) In-plane and edge-cleaved views of our crystals, respectively. Crystal orientation is obtained through X-ray diffraction. (c) In-plane Brillouin zone points. (d-g) In-plane isoenergy ARPES plots at energies from E_F to -3 eV. The k_y direction is parallel to the cleaved surface (panel b) so is covered by varying the emission angle. The k_x direction is normal to the edge-cleaved surface and is covered by varying the incident photon energy from 30 eV (low k_x) to 138 eV (higher k_x). The solid line representing 86 eV cuts through the K/H Brillouin zone point.

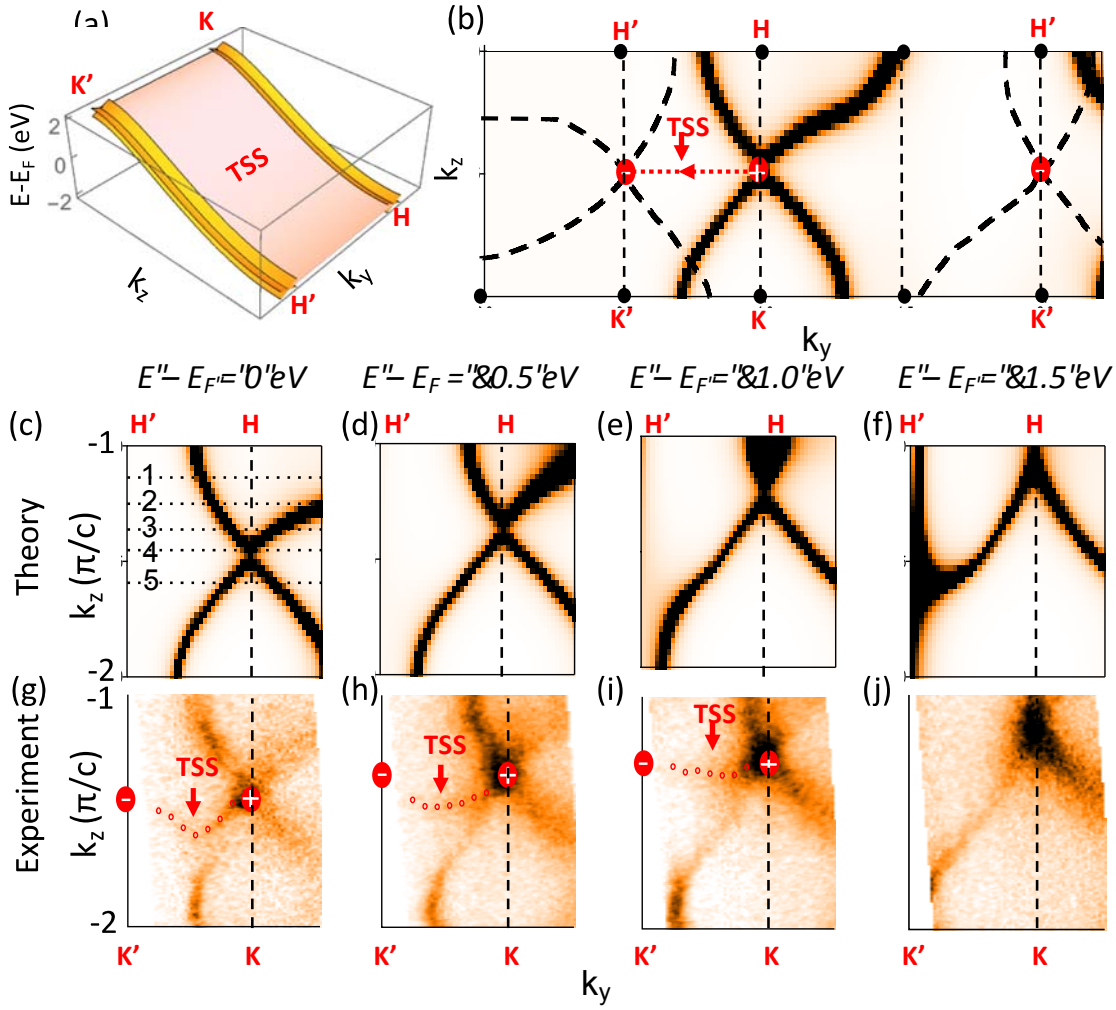

Fig 3. a) An illustration of how the 2D topological "water-slide" surface state (light magenta sheet) connects the 1D nodal lines. b) Illustration the K/H and K'/H' Dirac nodal lines with the Z_2 Berry phase monopoles (+ and -) projected to the 2D cleaved surface. The plot is made for the photon energy 86 eV ($k_x \approx 4$ in the units of figure 2c) that due to the proper k_x value can access the bulk Fermi surface in the center of the plot. The dashed bulk Fermi surface shown at the left and right are at incorrect k_x values to be observed. A topological surface state connecting the +1 and -1 monopoles on the projected surface Brillouin zone is drawn in by hand. (c-f) DFT spectral function convoluted by a Gaussian function (to simulate band broadening) in the k_y-k_z plane at 86 eV at a variety of binding energies. (g-j) Experimentally measured isoenergy contours using 86 eV photons. In addition to the excellent agreement between the predicted and measured bulk states, we identified an additional set of surface states (open circles) through Lorentzian fitting of momentum distribution curves along k_z (see Supplementary material[25] Fig.

S3). This surface state connects the pairs of Dirac points as predicted; therefore it is labeled as TSS (Topological Surface State or surface Fermi arc). The weak spectral intensity of the surface states is expected for a surface with cleavage imperfections or disorder.

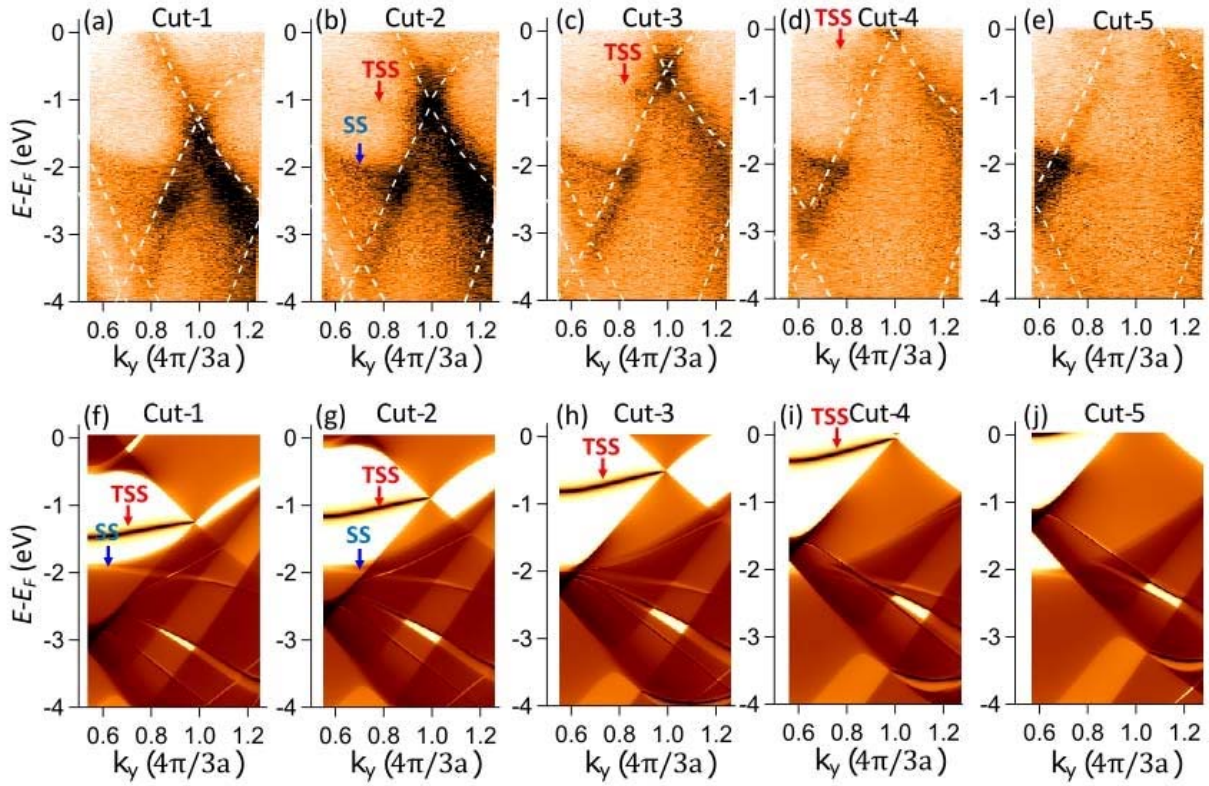

Fig. 4 Topological Surface States (TSS's) emanating from Dirac points. (a-e) ARPES spectra from the five cuts of Fig 3c, overlapped by DFT calculations (white dashed lines). The Dirac band crossings evolve from below E_F to above E_F consistent with the diagram of Fig 1d. Through second derivative analysis (see supplementary information[25] Fig. S4), we identified nearly flat topological surface states (red open circles) in cuts (b-d), which connects to the Dirac points and similarly moves up in energy. In contrast, regular (non-topological) surface states (indicated by the blue arrows) remains relatively "static" in energy in all 5 cuts. (f-j) DFT simulation of spectral intensity, convolved by a Gaussian function to simulate band broadening. The calculated DFT points have been shifted up by 0.5 eV relative to the measured spectra.